

Ultra-low-phase-noise cryocooled microwave dielectric-sapphire-resonator oscillators with frequency instability below 1×10^{-16}

John G. Hartnett,¹ Nitin R. Nand,¹ and Chuan Lu^{2*}

¹*School of Physics, University of Western Australia, 35 Stirling Hwy, Crawley 6009 WA, Australia*

²*School of Information Science and Technology, West Campus,*

University of Science and Technology of China, Hefei, Anhui, 230027, P.R. China

(Dated: March 20, 2019)

Two nominally identical ultra-stable cryogenic microwave oscillators are compared. Each incorporates a dielectric-sapphire resonator cooled to near 6 K in an ultra-low vibration cryostat using a low-vibration pulse-tube cryocooler. The phase noise for a single oscillator is measured at -105 dBc/Hz at 1 Hz offset on the 11.2 GHz carrier. The oscillator fractional frequency stability is characterized in terms of Allan deviation by $5.3 \times 10^{-16} \tau^{-1/2} + 9 \times 10^{-17}$ for integration times $0.1 \text{ s} < \tau < 100 \text{ s}$ and is limited by a flicker frequency noise floor below 1×10^{-16} .

PACS numbers: 77.90.+k, 65.40.-b, 06.30.Ft, 07.20.Mc

The time and frequency standards community is ever advancing the state-of-the-art in both stability and accuracy of atomic clocks [1]. With the development of atomic fountain clocks it was found that a more stable microwave interrogation oscillator was required than was available from an ultra-stable quartz oscillator to avoid the Dick effect [2–5]. The latter results from the fact that most atomic fountain clocks have significant dead time in their interrogation cycle, simply due to the fact that they are pulsed devices where one has to wait until the detection process is finished before the next cloud of cold atoms is launched [6]. This results in the introduction of the phase noise of the local reference oscillator, from which the microwave cavity frequency is derived, to the short-term stability of the fountain clock. The problem was overcome through the use of cryogenic sapphire oscillators with significantly much better short-term frequency stability [8] and as a result it has resulted in atomic fountain clocks reaching a performance limited only by quantum projection noise [7].

These microwave oscillators based on a dielectric-sapphire resonator cryogenically cooled to nearly 6 K are in use in several standards labs and have been found to be useful for various applications [9–12]. The oscillators, [13–15] until recently, have relied on large dewars of liquid helium to cool the resonator with a few exceptions [16–19] where a cryocooler was used. However the latter had their short-term performance compromised by vibrations from the cryocooler itself. More recently low vibration pulse-tube cryocoolers and specially designed cryostats [20] have enabled cryogenic oscillators as equally stable [21–25] yet without being limited by the noise from the cryocooler.

The present design is currently state-of-the-art. A silver-plated copper cavity encloses a 51 mm diameter and 30 mm high HEMEX grade sapphire cylindrical resonator and is the same as previously reported [13] (see

Fig. 1 therein) but the thermal design for housing it in the cryostat is significantly different [24]. See Fig. 1. Also long coaxial cables connecting the cryogenic resonator to the room temperature loop oscillator (feedback amplifier and microwave electronics) are no longer used as the cryostat is very compact and as a result the oscillator does not suffer from a slowly decreasing level of liquid helium as it does in the case with large liquid helium dewars. The cryostat [20] uses only about one liter of liquid helium that is constantly reliquified in a closed system by the low-vibration cold head. There is no hard contact between the cold head and the dielectric resonator resulting in significant reduction in vibrations and an enhanced temperature stability at the resonator due to specially engineered thermal filtering.

Two separate cryogenic oscillators were implemented with output frequencies near 11.2 GHz but differing by 1.58 MHz. At the control temperature for each resonator near 6 K, the resonators have loaded Q-factors of 1 billion and primary coupling better than 0.8 via loop probes made from the coaxial lines connecting to the room temperature loop oscillator. This paper reports on the inferred phase noise and frequency stability of a single oscillator by comparing two nominally identical and independent oscillators using this type of cryostat and pulse-tube cryocooler. Previously comparisons were made against a second oscillator using a large liquid helium dewar.

In order to compare the oscillators which output at slightly different microwave frequencies near 11.2 GHz a technique was implemented that could measure both their phase noise and frequency stability in real-time. With this technique the noise performance of the oscillators could be easily optimized and it was discovered that at much lower power levels incident on the resonator than had previously been used better frequency stability could be achieved.

An oscillator can be considered as a resonator driven by an amplifier of noise temperature T_N . Thermal noise induces fractional frequency fluctuations according to, $\Delta f/f_T = (kT_N/2P_{inc}Q^2\tau)^{1/2}$, the Townes-Schawlow formula where τ is the integration time of the mea-

*Electronic address: john.hartnett@uwa.edu.au

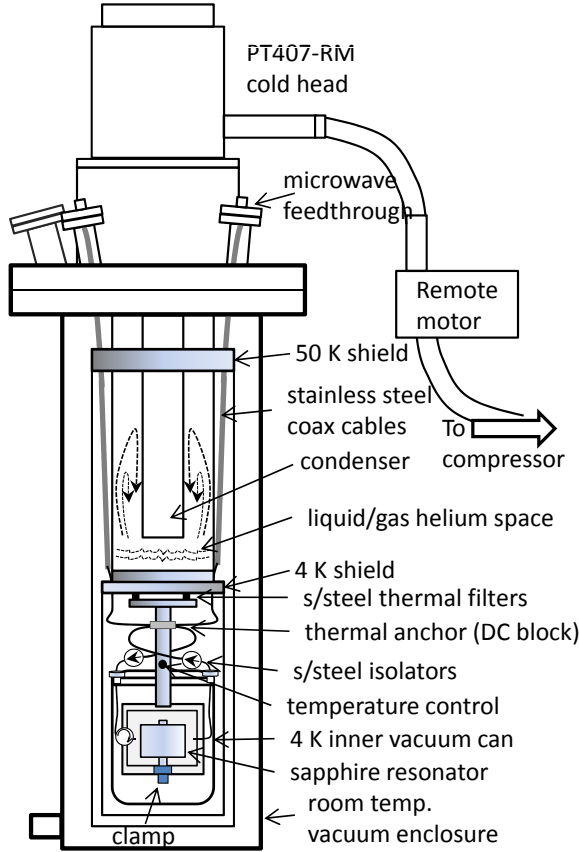


FIG. 1: A schematic diagram of the CryoMech low-vibration cryostat [20] housing the sapphire resonator on the cold finger cooled by about a liter of liquid helium in the enclosed liquid/gas helium space. The CryoMech PT407-RM pulse-tube condenser constantly maintains the liquid helium bath near 4 K. A heater, sensor and a Lakeshore 340 temperature controller maintains the temperature at the sapphire crystal within about $10 \mu\text{K}$ in the short-term by controlling the temperature at the frequency-temperature turnover point.

surement, P_{inc} the power incident on the resonator and Q the resonator quality factor. Yet fractional frequency fluctuations due to radiation pressure $\Delta f/f_P \propto (Q/f)(P_{inc}hf/\tau)^{1/2}$. There is an optimal power level P_{opt} where these competing effects on frequency fluctuations are equal and hence frequency fluctuations are minimized [26]. By lowering the power incident on the resonator $P_{opt} = 0.1 \text{ mW}$ was found after which any further reduction in power caused the oscillator stability to deteriorate due to increased thermal fluctuations. The analysis also indicates the possibility for a microwave oscillator to reach a short-term fractional frequency stability below 1×10^{-16} .

Experimental Method— A block diagram of the measurement technique which enabled simultaneous measurement of the relative phase noise and frequency stability of two cryocooled oscillators is shown in Fig. 2. The 11.201967 GHz signal from one of the cryogenic oscillators was split via a 3-dB power splitter and one of the outputs was down-converted to approximately 100 MHz

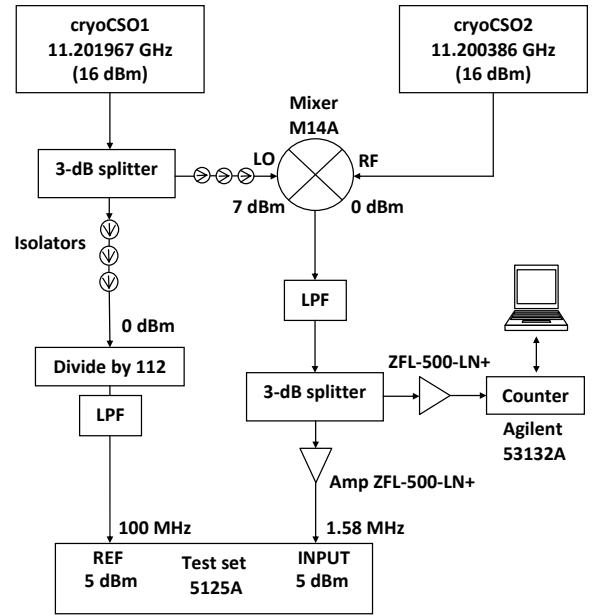


FIG. 2: A block diagram of the measurement technique used to compare two cryocooled oscillators (cryoCSO1 and cryoCSO2) with a Symmetricom 5125A phase noise test set (attenuators and DC blocks not shown). The principle components used were; a Watkins Johnson M14A mixer, Mini-Circuits amplifiers ZFL-500LN+, and a divide by 112 chain. The latter was constructed from the series connection of Hit-tite dividers: the HMC364 divide by 2, the HMC365 divide by 4, and the HMC705LP4 programmable divider which was set to divide by 14. LPF = Low Pass Filter.

via a 112 divider chain. The chain was constructed from the series connection of three low noise dividers (divide by 2 then divide by 4 then divide by 14). The 100 MHz output was then used as the very low phase noise reference signal in a Symmetricom 5125A test set. The input signal to the test set is the 1.58 MHz beat note of the two oscillators.

The test set outputs the single sideband (SSB) phase noise $\mathcal{L}_\varphi(f)$ in dBc/Hz and the Allan deviation of the fractional frequency stability of the input signal relative to the reference signal. The test set performs phase detection by sampling the RF waveforms directly using digital signal processing methods [27]. The particular model test used has an frequency input range from 1 MHz to 400 MHz, therefore it was necessary to down-convert from the microwave frequency to enable the comparison. In addition the beat note was also sampled with an Agilent 53132A universal frequency counter with a gate time of 10 s, and a computer controlled data acquisition system.

From a prior comparison of one cryocooled sapphire oscillator with a liquid helium cooled version it was expected that the phase noise for a single oscillator would be about -97 dBc/Hz at 1 Hz offset [23]. Dividing down the 11.2 GHz frequency by the factor 112 means a further 41 dB reduction in phase noise and hence that for the 100 MHz reference from the output of the divider

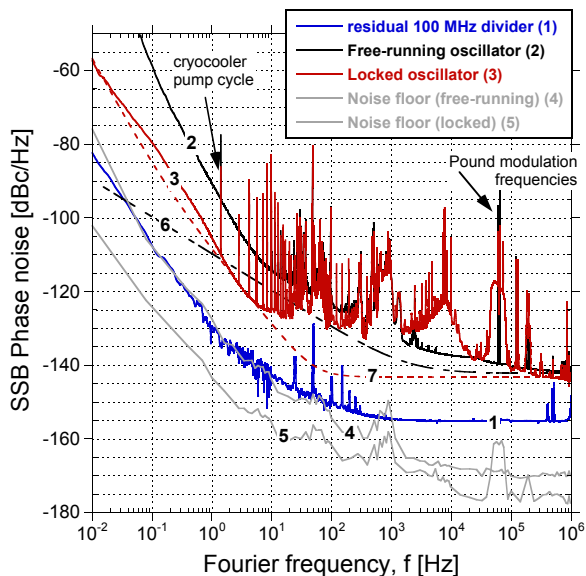


FIG. 3: (color online) The residual SSB phase noise of the 100 MHz divider chain (curve 1), and the SSB phase noise for a single oscillator (at 11.2 GHz) without (free-running, curve 2) and with the Pound frequency control and power control servos engaged (locked, curve 3) where the power incident on the resonator $P_{inc} = 0.1$ mW. Curve 4 and 5 are the measurement noise floors for the free-running and locked oscillators measurements. Curve 6 represents the phase noise at 11.2 GHz of the Endwave JCA microwave amplifier used in the loop oscillator, measured with an incident power level of -30 dBm, which is the loop oscillator operating condition. Curve 7 is a best fit for the phase noise of the locked oscillator for Fourier frequencies $f < 10$ Hz.

chain is dominated by the residual phase noise of the dividers themselves. Using two nominally identical divider chains their residual phase noise was measured to be -130 dBc/Hz at 1 Hz offset (see curve 1 of Fig. 3). This is about 30 dB lower than the phase noise of 11.2 GHz signal of the microwave oscillator.

Results and discussion— Fig. 3 shows the measured SSB phase noise of a single cryocooled sapphire oscillator where the incident power on the resonator $P_{inc} = 0.1$ mW. It is shown for the case where the oscillators are free-running (curve 2) and when the Pound frequency control and power control servos are engaged (curve 3). Curve 6 describes the measured phase noise of the high gain microwave amplifier used in the loop oscillator, with an input power into the amplifier of -30 dBm, which is the loop operating condition. The phase noise for a single oscillator, at Fourier frequencies $f < 10$ Hz, can be approximately described by the fit (curve 7) in Fig. 3, given by

$$\mathcal{L}_\varphi(f) = 10 \log \left(\frac{10^{-11.7}}{f^3} + \frac{10^{-10.9}}{f^2} + 10^{-14.3} \right). \quad (1)$$

This is characteristic of white frequency ($1/f^2$) noise at Fourier frequencies $f < 10$ Hz and flicker frequency noise

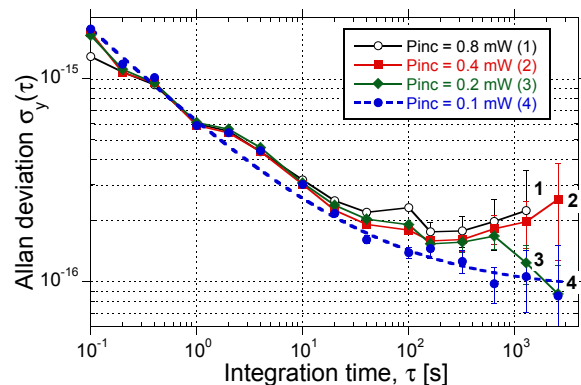


FIG. 4: (color online) Allan deviation $\sigma_y(\tau)$ for a single cryocooled sapphire oscillator as a function of integration time τ . The legend indicates the incident power on the resonator (P_{inc}). Curves 1 to 3 result from points joined as a guide to the eye. Curve 4 is a curve fit described by Eq. (2).

at much lower frequencies. The measured SSB phase noise of -105 dBc/Hz at 1 Hz offset is state-of-the-art for any microwave oscillator, only 5 dB above that of the microwave amplifier. Outside the bandwidth of the Pound frequency control servo (of several hundred Hz) the oscillator is limited by the phase noise of the microwave amplifier which reaches a thermal phase noise floor near -143 dBc/Hz at Fourier frequencies $f > 10^5$ Hz. The spurs seen in Fig. 2 are due to the 1.41 Hz cryocooler compressor cycle frequency, the 50 Hz mains power, and their harmonics. They are seen in part due to poor rejection by the measurement equipment.

The oscillator frequency stability was evaluated for various levels of microwave power (P_{inc}) incident on the cryogenic resonator in the range 0.1 mW to 0.8 mW. Fig. 4 shows the frequency stability for a single oscillator, in terms of Allan deviation ($\sigma_y(\tau)$), after a linear fractional frequency drift of about 4.4×10^{-14} /day was subtracted, and data collected for at least 3 hours. At the time oscillators had been running for only between 1 to 2 weeks. At 1-s integration time $\sigma_y = 5.8 \times 10^{-16}$, a robust result and repeatable over many hours to days of measurement and independent of incident power over the range shown. For incident power $P_{inc} = 0.1$ mW (curve 4) the oscillator instability is minimized and can be described by,

$$\sigma_y(\tau) = 5.3 \times 10^{-16} \tau^{-1/2} + 9 \times 10^{-17}. \quad (2)$$

For integration times $0.1 < \tau < 100$ s, the stability is white frequency noise limited, with a flicker frequency floor below 1×10^{-16} . Reducing the power further only degraded the stability due to an increase in thermal noise.

However, there is a flicker frequency noise floor dependent on incident power. From Fig. 4 it may be noted at the larger integration times there is a trend of improved stability with decreasing incident power. By taking the quadratic differences between curves 1 to 3, respectively, and curve 4 according to

$$(\Delta\sigma_y^2(\tau))^{1/2} = (\sigma_y^2(\tau)_x - \sigma_y^2(\tau)_{0.1})^{1/2}, \quad (3)$$

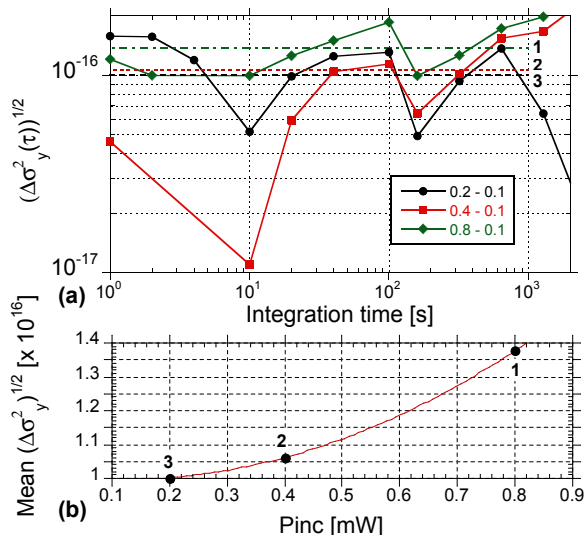


FIG. 5: (color online) (a) The quadratic differences in the Allan deviation $((\Delta\sigma_y^2(\tau))^{1/2})$ for the curves of Fig. 4 subtracted from $\sigma_y(\tau)$ at $P_{inc} = 0.1$ mW (curve 4 of Fig. 4) as a function of integration time τ . The legend indicates the incident power (P_{inc} in mW) for the respective curves from which the curve for $P_{inc} = 0.1$ mW has been subtracted. (b) The mean values of the $(\Delta\sigma_y^2(\tau))^{1/2}$ data for each curve in Fig. 5(a) with corresponding numbers.

where subscript x indicates σ_y where $P_{inc} = 0.8, 0.4$ and 0.2 mW, corresponding to curves 1, 2 and 3 in Fig. 4 and the subscript 0.1 indicates σ_y where $P_{inc} = 0.1$ mW, corresponding to curve 4. The results are shown in Fig. 5(a). There is a lot of scatter in the data due to the large

uncertainties coming from differencing similar sized numbers and the nature of the statistics of the noise. Nevertheless the results indicate the presence of a flicker floor that is power dependent. The horizontal lines labeled 1 to 3 are the best fit mean values. These are shown in Fig. 5(b) as a function of the P_{inc} value for $\sigma_y(\tau)_x$ in Eq. (3). The curve drawn through these points is the best fit quadratic which when extrapolated to $P_{inc} = 0.1$ mW represents a flicker floor contribution to the oscillator stability just below 1×10^{-16} . This is also consistent with the best fit (curve 4) in Fig. 4 to the $\sigma_y(\tau)$ data where $P_{inc} = 0.1$ mW. From that a flicker floor of about 9×10^{-17} is indicated.

In conclusion, two nominally identical cryocooled sapphire oscillators where the resonator is cooled to near 6 K with an ultra-low vibration pulse-tube cryocooler and custom built cryostat have been realized and compared. The fractional frequency stability for a single oscillator is 5.8×10^{-16} for an integration time of 1 s reducing according to a white frequency power law ($\tau^{-1/2}$) to a flicker frequency floor below 1×10^{-16} . The frequency stability is minimized at an optimal level of incident power on the cryogenic resonator. This is consistent with a reduction of radiation pressure on the crystal wall to a level where its contribution to the oscillator frequency stability is equal to the thermal noise contribution. And the presence of a power dependent flicker floor indicates some noise process originating in the cryogenic resonator itself.

This work was supported by Australian Research Council grants LP0883292 and DP1092690. The authors thank E. Ivanov, M. Nagel and E. Kovalchuk for their helpful suggestions.

-
- [1] J.G. Hartnett and A.N. Luiten, *Rev. Mod. Phys.*, **83**, 1 (2011).
- [2] G.J. Dick, *Proc. 19th Ann. PTTI Systems and Applications Meeting (Redondo Beach, CA)*, 133 (1987).
- [3] G.J. Dick *et al.*, *Proc. 22th Ann. PTTI Systems and Applications Meeting (Vienna)*, 497 (1990).
- [4] C. Audoin *et al.*, *IEEE Trans. Ultrason. Ferro. Freq. Contr.*, **45**, 877 (1998).
- [5] G. Santarelli *et al.*, *IEEE Trans. Ultrason. Ferro. Freq. Control* **45**, 887 (1998).
- [6] R. Wynands and S. Weyers, *Metrologia*, **42**, S64 (2005).
- [7] G. Santarelli *et al.*, *Phys. Rev. Lett.*, **82**, 4619 (1999).
- [8] S. Chang *et al.*, *Electron. Lett.*, **36**, 480 (2000).
- [9] P. Wolf *et al.*, *Phys. Rev. D* **70**, 051902 (2004).
- [10] P. Stanwix *et al.*, *Phys. Rev. Lett.* **95**, 040404 (2005).
- [11] G. Marra *et al.*, *Meas. Sci. Technol.*, **18**, 1224 (2007).
- [12] K. Watabe *et al.*, *CPEM Special Issue IEEE Trans on Instr. Meas.*, **56**, 632 (2007).
- [13] J.G. Hartnett *et al.*, *Appl. Phys. Lett.*, **89**, 203513 (2006).
- [14] M.E. Tobar *et al.*, *IEEE Trans. Ultrason. Ferro. Freq. Contr.*, **53**, 2386 (2006).
- [15] C.R. Locke *et al.*, *Rev. Sci. Instr.*, **79**, 051301 (2008).
- [16] G. J. Dick and R. T. Wang, in *Proc. 2000 Int. IEEE Freq. Contr. Symp.*, 480 (2000).
- [17] R.T. Wang *et al.*, in *Proc. 2004 IEEE Int. Freq. Contr. Symp.*, 752 (2004)
- [18] K. Watabe *et al.*, in *Proc. 2003 IEEE Int. Freq. Contr. Symp.*, 388 (2003).
- [19] K. Watabe *et al.*, *IEICE Trans. Elect.* **E87-C**, 1640 (2004).
- [20] C. Wang and J.G. Hartnett, *Cryogenics*, **50**, 336 (2010).
- [21] S. Grop *et al.*, *Rev. Sci. Instr.*, **81**, 025102 (2010);
- [22] S. Grop *et al.*, *Elect. Lett.*, **46**, 420 (2010).
- [23] J.G. Hartnett *et al.*, *IEEE Trans. Ultrason. Ferroelect. Freq. Control*, **57**, 1034 (2010).
- [24] J.G. Hartnett and N.R. Nand, *IEEE Trans. Microw. Theory Tech.*, **58**, 3580 (2010).
- [25] N.R. Nand *et al.*, *IEEE Trans. Microw. Theory and Tech.*, **59**, 2978 (2011).
- [26] S. Chang *et al.*, *Phys. Rev. Lett.* **79**, 2141 (1997).
- [27] S. Stein, *IEEE Trans. Ultras. Ferro. Freq. Contr.*, **57**(3), 540 (2010).